MDR1 function is sensitive to the phosphorylation state of myosin regulatory light chain

Gaurav Bajaj, Rosita Rodriguez-Proteau, Anand Venkataraman, Ying Fan, Chrissa Kioussi, Jane E. Ishmael *

Department of Pharmaceutical Sciences, College of Pharmacy, Oregon State University, Corvallis, OR 97331, USA

ARTICLE INFO

ABSTRACT

Multiple drug resistance protein 1 (MDR1) is composed of two homologous halves separated by an intracellular linker region. The linker has been reported to bind myosin regulatory light chain (RLC), but it is not clear how this can occur in the context of a myosin II complex. We characterized MDR1-RLC interactions and determined that binding occurs via the amino terminal of the RLC, a domain that typically binds myosin heavy chain. MDR1-RLC interactions were sensitive to the phosphorylation state of the light chain in that phosphorylation by myosin light chain kinase (MLCK) resulted in a loss of binding in vitro. We used ML-7, a specific inhibitor of MLCK, to study the functional consequences of disrupting RLC phosphorylation in intact cells. Pretreatment of polarized Madin–Darby canine kidney cells stably expressing MDR1 with ML-7 produced a significant increase in apical to basal permeability and a corresponding decrease in the efflux ratio (threefold; $p < 0.01$) of [^{3}H]-digoxin, a classic MDR1 substrate. Together these data show that MDR1-mediated transport of [^{3}H]-digoxin can be modulated by pharmacological manipulation of myosin RLC, but direct MDR1-RLC interactions are atypical and not explained by the structure of the myosin II holoenzyme.

1. Introduction

MDR protein 1 (MDR1), also known as P-glycoprotein or ABCB1, is the prototypical ATP-binding cassette (ABC) efflux transporter associated with drug resistance. MDR1 has two halves, each consisting of six membrane-spanning domains plus a nucleotide binding domain, joined by a linker region [1–4]. The intracellular linker is approximately seventy-five amino acids and is essential to both the transport function and ATPase activity of MDR1 [3,5]. The study of ABC transporters in a variety of cell types suggests that the linker is also a determinant of cell surface expression [3,6,7]. Identification of several cytoskeletal, regulatory and motor proteins as direct binding partners of the linker domain has continued to support this idea [4,6,8,9]. For example, linker-interacting proteins such as HAX-1 and myosin RLC have been implicated in clathrin-mediated endocytosis and apical trafficking of bile salt export protein (BSEP), respectively [6,9].

The identification of myosin RLC as a binding partner of several ABC transporters, including MDR1 [9], was intriguing as we had independently identified the same light chain as a direct binding partner of subunits belonging to the N-methyl-ᴅ-aspartate (NMDA) family of glutamate-gated ion channels [10,11]. Myosin RLC is regarded as an integral component of myosin II, a hexameric complex that contributes to cell motility, adhesion, shape and polarity in nonmuscle cells [12], that has also been implicated in short-range, actin-based trafficking events [13–17]. Myosin RLC-NMDA receptor interactions serve a trafficking function but do not tether the NMDA receptor directly to the myosin II motor complex [18]. As the disposition of RLC in binding other interacting partners has not been determined [6,19,20], we characterized the domains required for interaction with the linker region of MDR1 and investigated the consequences of disrupting MDR1-RLC interactions in whole cells.

2. Materials and methods

2.1. DNA constructs and proteins

A fragment encoding the linker region (amino acid residues 633–709) of human MDR1 (GenBank accession No. M14758) was amplified by PCR and inserted into pGEX-6P-3 (GE Healthcare Bio-Sciences Corp., Piscataway, NJ). Full-length and mutant RLC in pET28a (Novagen, Madison, WI), and the C-terminus of NMDAR1 (834–938) in pGEX-2T have been described previously [10,18]. The C-terminus of the acid-sensing ion channel (ASIC) 2a in pGEX-6P-3 was the gift of Dr. Julie Saugstad (Robert S. Dow Neurobiology Laboratories, Portland, OR). Recombinant pET28a/MRLC was expressed in Escherichia coli (BL21-Gold(DE3)pLysS; Stratagene, La Jolla, CA), and purified by nickel chelate chromatography as described

* Corresponding author. Fax: +1 541 737 3999.
E-mail address: jane.ishmael@oregonstate.edu (J.E. Ishmael).

previously [18]. Purified light chain was phosphorylated in the presence of smooth muscle 10 µg/ml MLCK [18] and phosphorylation verified by polyacrylamide gel electrophoresis (PAGE) against either non-phosphorylated or mock phosphorylated samples. Samples were heated at 80 °C for 2 min in urea sample buffer (8 M urea, 33 mM Tris–glycine pH 8.6, 0,17 mM EDTA and bromophenol blue), and resolved on NOVEX Tris–glycine pre-cast gels (Invitrogen, Carlsbad, CA). Protein was visualized directly by Coomassie blue stain (BioRad Laboratories, Hercules, CA), or electro-transferred to nitrocellulose membrane (Amersham Bio-sciences, Piscataway, NJ) and detected by immunoblot analysis using a chemiluminescence assay for detection (Roche, Indianapolis, IN).

2.2. Chemicals and reagents

Radiolabelled [3H]-digoxin (23.4 Ci/mmol, >97% purity) was obtained from Amersham, Inc. (Piscataway, NJ). 1-(5-Iodonaphthalene-1-sulfonyl)-1H-hexahydro-1,4-diazepine hydrochloride (ML-7), verapamil and digoxin were purchased from Sigma, Inc. (St Louis, MO). For in vitro phosphorylation reactions, calmodulin was purchased from Calbiochem (San Diego, CA) and smooth muscle MLCK was a kind gift from Dr. Sonia Anderson (Oregon State University, Corvallis, OR). All stock solutions were prepared on the day of the experiment; final concentrations of DMSO or ethanol did not exceed 0.1% v/v or 0.5% v/v for ML-7 and verapamil, respectively. Anti-myosin RLC antibodies αMRLC/3 [10] and αMRLC/P [18] have been described previously. Additional primary antibodies were from commercial sources and included: anti-MDR1 (anti-ABCB1 MAb/ C219; Axxora, LLC, San Diego, CA) and anti-T7 (Novagen, Madison, WI).

2.3. Glutathione-S-transferase (GST) pull-down assays

Regions of MDR1, NMDAR1 or ASIC2a fused to GST were expressed in E. coli (BL21-Gold(DE3)pLysS) and tested for their ability to interact with either recombinant myosin RLC or native myosin RLC derived from mouse brain in the absence of added magnesium [10,18]. For pull-down assays from brain homogenates, cerebral cortices were pooled from three adult Swiss Webster mice and homogenized in a buffer containing (150 mM NaCl, 25 mM Tris, 5 mM EDTA, 5 mM EGTA, 10 mM ATP, 5 mM DTT). Assays were initiated by the addition of soluble cortical protein (1 mg) and incubated with gentle rotation overnight at 4 °C. Unbound proteins were removed by three sequential washes with binding buffer and bound proteins then eluted from the beads by boiling in sample buffer. Proteins were separated by sodium-dodecyl sulfate (SDS)–PAGE, and transferred to nitrocellulose membranes for immunoblot analyses. Recombinant myosin RLC was detected with either an anti-T7-tag antibody (RLC) or αMRLC/P. Native myosin RLC was detected with αMRLC/3.

2.4. Transepithelial transport studies

MDCK cells stably expressing human MDR1 (MDCKII-MDR1), a kind gift from Dr. Piet Borst (The Netherlands Cancer Research Institute), were maintained in Dulbecco's Modified Eagle Medium (DMEM; Gibco, Grand Island, NY) with 10% fetal bovine serum (Hyclone; Logan, UT), plus 0.01% penicillin/streptomycin. For transport studies, cells were grown (3×10^5 cells/well) on Transwell® (Corning) inserts (4.71 cm²), and maintained for 3 days after confluency to allow polarization. Inserts were washed three times with transport buffer (Hanks' Buffered Salt Solution (HBSS) containing 10 mM HEPES and 25 mM D-glucose), and allowed to equilibrate for 30 min before assessment of monolayer integrity using a World Precision Instrument (Sarasota, FL). Transepithelial electrical resistance (TEER) values were determined for each monolayer, by subtracting the resistance of blank inserts and correcting for surface area. Only cultures with resistance >500 Ω cm², indicating formation of tight junctions, were used. The effect of pharmacologecal inhibitors was assessed by pre-treating monolayers with drug or vehicle for up to 4 h before initiation of transport studies. There was no significant difference between TEER values taken before and after treatment (data not shown), indicating that the integrity of cell monolayers was not compromised by drug exposure.

Transport studies were conducted at 37 °C in air, 5% CO₂ and 95% relative humidity with [3H]-digoxin (1 µCi; 0.5 µM) in transport buffer at pH 6.8 for the apical (AP) and pH 7.4 for the basolateral (BL) compartment. [3H]-Digoxin transport was assessed in both AP to BL and BL to AP directions. Aliquots (100 µl) were initially taken from the donor and receiver chambers, and thereafter from the receiver chamber every 30 min up to 3.0 h. The entire receiving compartment was replaced with a fresh solution of HBSS at each time interval. Aliquots were placed in 0.9 ml scintillation fluid (Cytoscint ES, ICN, Cosa Mesa, CA) and [3H]-activity measured on a Beckman LS 6500 scintillation counter (Palo Alto, CA). The effective permeability coefficients (P_e) of digoxin after every 30 min were calculated using the following equation [21]:

$$P_e = V_d \times \Delta\%/A \times \Delta t$$

where P_e is the effective permeability coefficient (cm s^{-1}), V_d is the volume (cm³) of the donor compartment, A is the surface area of the monolayer (4.71 cm²), and $\Delta\%/\Delta t$ is the percentage mass transported (s^{-1}). The apparent permeability (P_{app}) of digoxin after 3 h was subsequently calculated using the following equation [22]:

$$P_{app} = dQ/dt \times 1/(A \times C_0)$$

where A is the surface area of the monolayer (4.71 cm²), C_0 is the initial concentration of radiolabelled probe substrate in the donor compartment; and dQ/dt is the slope of the steady-state rate constant.

The efflux ratio was determined by dividing P_{app} in the BL to AP direction by P_{app} in the AP to BL direction

$$\text{Efflux ratio} = \frac{P_{app}(BL \to AP)}{P_{app}(AP \to BL)}$$

2.5. Statistical analysis of transport data

Values are presented as mean ± standard error (SE). Differences in AP and BL permeability, TEER readings and efflux ratios of treatment groups were compared with respective controls using an unpaired t-test. Differences in TEER readings within various treatment groups were compared using one-way ANOVA followed by Bonferroni's multiple comparison test. Statistical significance was represented as: **$p < 0.01$, *$p < 0.05$.

3. Results and discussion

3.1. Myosin RLC is a direct binding partner of MDR1

We compared the ability of myosin RLC to bind target sequences from seemingly unrelated membrane-bound proteins (Fig. 1A). For these studies the intracellular linker region of MDR1, the full-length C-terminus of NMDAR1, and the C-terminus of an unrelated ion channel subunit, ASIC2a, were expressed in bacteria as GST fusion proteins and immobilized on glutathione-Sepharose beads. Immobilized GST fusion proteins were used as affinity matrices to examine interactions with either recombinant myosin RLC (Fig. 1B, upper panel), or native light chain derived from mouse cortex (Fig. 1B, lower panel). Purified myosin RLC bound strongly and specifically to GST/MDR1 linker and NMDAR1 C-terminus (NR1-C), yet failed to interact with GST alone or a GST/ASIC2a (lanes 2 and 3, Fig. 1B, upper panel). A
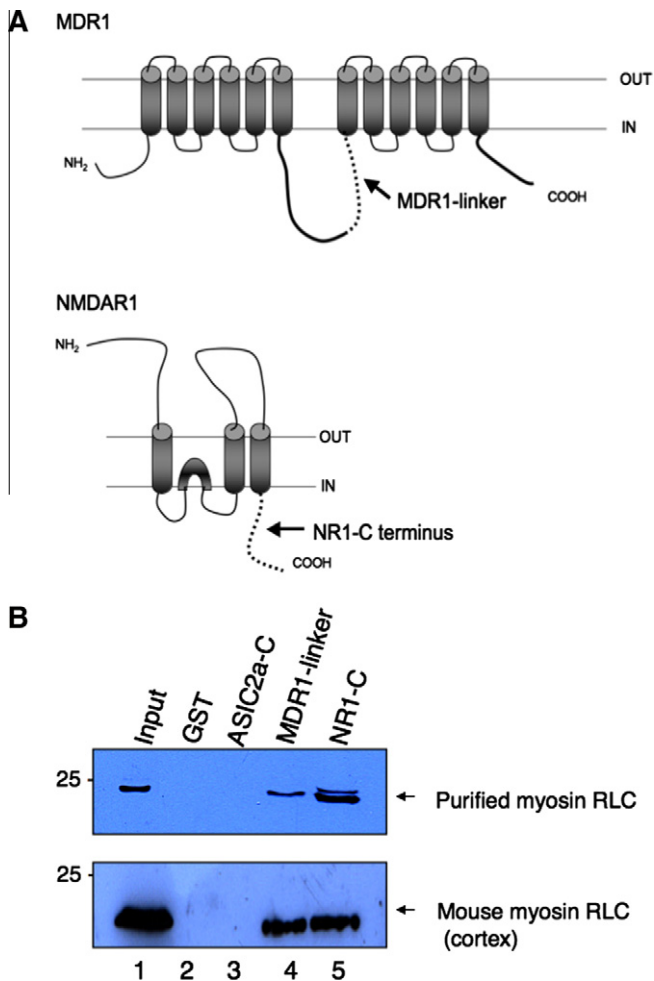
Fig. 1. Myosin RLC binds directly to the linker region of human MDR1. (A) Schematic representation of the membrane topology of MDR1 and the NMDAR1 subunit of the NMDA receptor showing intracellular myosin RLC binding domains. (B) Recombinant and native RLC were retained on affinity matrices corresponding to the MDR1-linker region and C-terminus of NMDAR1 (NR1-C), but not on affinity matrices corresponding to GST alone or the C-terminus of acid-sensing ion channel (ASIC) 2a. Autoradiographs are representative of three (purified RLC) or four independent determinations (brain homogenates for each experiment were prepared from four independent animals).

Fig. 2. Myosin RLC binds to the linker region of MDR1 via the amino terminal of the light chain. (A) Schematic representation of a series of HA-tagged myosin RLC deletion mutants (corresponding to amino acids 1–101, 61–129, 102–172, 1–129, 61–172) used in panel B. (B) A truncated recombinant myosin RLC (amino acids 1–129) was sufficient for binding directly to the MDR1-linker region (compare lanes 9 and 15). The amino terminal region (1–101) was retained but to a lesser extent than wild-type myosin RLC (compare lanes 3 and 15). Panel B is representative of three independent determinations.

similar pattern of binding was observed in GST pull-down assays where purified myosin RLC was substituted for homogenates derived from mouse cortex (Fig. 1B, lower panel). Immunoblotting with an anti-myosin RLC antibody revealed that mouse brain myosin RLC was retained on GST affinity matrices containing the MDR1 linker (lane 4, Fig. 1B, lower panel) and the NMDAR1 C terminus (lane 5, Fig. 1B, upper panel), yet did not bind to either GST alone (lane 2, Fig. 1B, lower panel) or GST/ASIC2a (lane 3, Fig. 1B, lower panel). These data indicate that myosin RLC is a direct binding partner of at least two integral membrane proteins.

3.2. The amino terminal of myosin RLC is required for binding MDR1

To determine the structural basis of light chain interactions with MDR1 we expressed deletion mutants of RLC in bacteria and examined them for interaction with the MDR1 linker domain (Fig. 2). The RLC mutant corresponding to the first three helix–loop–helix motifs (EF-hand domains) of the protein (1–129) bound to GST/MDR1 in a manner that was comparable to that of the full-length (1–172) protein (compare lanes 9 and 15 of Fig. 2, panel B). The RLC mutant lacking the third EF-hand domain (1–101) was also
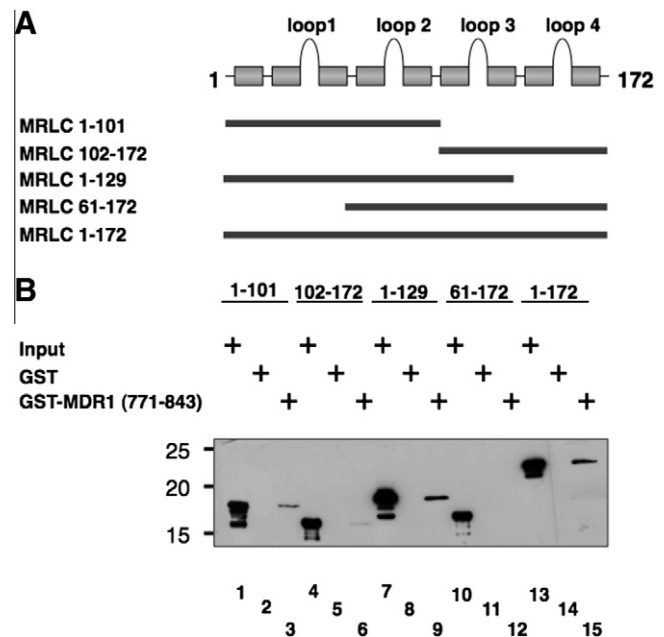
retained, albeit to a lesser extent, on a GST/MDR1 affinity matrix (lane 3 of panel B). Deletion of the first one or two EF-hand domain of the light chain (to yield either 61–172 or 102–172, respectively) dramatically reduced or abolished the interaction of RLC with GST/MDR1 (lanes 6 and 12 of panel B, respectively). These findings indicate that residues in the amino terminal of myosin RLC are critical for MDR1 binding. The first EF-hand domain is necessary for binding; residues between 61 and 129 of the light chain likely contribute to the overall stability of the protein–protein interaction whereas residues 130–172 are not part of the MDR1-RLC interface.

MDR1-RLC interactions were qualitatively similar to NMDA-RLC interactions [18], suggesting that the light chain likely adopts a similar conformation when bound. In contrast, and in keeping with the available crystal structures of the myosin II complex [23–25], all four EF-hand domains were previously found to be necessary for RLC binding to myosin II heavy chain and required magnesium [18]. The direct interaction between the RLC and MDR1 can therefore not be explained by the traditional interaction of myosin RLC as a component of the myosin II holoenzyme. Rather than forming a bridge between myosin II heavy chain and MDR1, myosin RLC likely forms a complex with MDR1 that is independent of the heavy chain. Such light chain-containing complexes have been described before for a *Saccharomyces cerevisiae* essential light chain, Mlc1p, during mitosis and serve to recruit the target protein to a specific subcellular, actin-rich compartment [26].

3.3. The phosphorylation state of myosin RLC is a critical determinant of MDR1-light chain binding

The amino terminal region of myosin RLC is phosphorylated by MLCK at Ser19 and Thr18 [27]. To determine if MDR1-RLC interactions are modulated by phosphorylation, a minimal RLC-interacting domain (residues 1–129) was phosphorylated *in vitro* by MLCK and tested for interaction with the MDR1 linker and the NMDAR1 C-ter-

minal (Fig. 3). Phosphorylation was confirmed following all *in vitro* reactions by immunoblot analysis of RLCs resolved by urea–glycerol PAGE (Fig. 3B). Phosphorylated and non-phosphorylated RLCs were examined in parallel for interaction with GST/MDR1 and GST alone (Fig. 3C), or GST/NR1-C and GST alone (Fig. 3D) using an antibody to both forms of the protein. In the phophorylated state myosin RLC (1–129) binding to either MDR1 (Fig. 3C), or NMDAR1 (Fig. 3D), was dramatically reduced when compared with non-phosphorylated RLC (lane 3 and 6, Fig. 3C and D). Loss of binding was confirmed by the use of a phospho-specific antibody that recognizes only the phosphorylated form of the RLC (data not shown). This pattern of binding was also observed when RLC (1–129) was substituted

Fig. 3. Myosin RLC-MDR1 interactions are sensitive to phosphorylation by myosin light chain kinase (MLCK). (A) Schematic representation of the truncated myosin RLC mutant (amino acids 1–129) used in panel C showing threonine and serine phosphorylation sites, respectively. (B) Phosphorylation of recombinant myosin RLC by MLCK was verified after each reaction by PAGE in 8 M urea followed by Coomassie staining to visualize recombinant proteins. Panel shows representative immunoblot analysis of myosin RLC (MRLC 1–129), before (lane 1) and after (lane 2) phosphorylation by MLCK *in vitro*. Gels were transferred to nitrocellulose membranes and proteins detected using an anti-T7 antibody. (C,D) GST/MDR1, GST/NR1-C or GST alone, were immobilized on glutathione-Sepharose beads and incubated with non-phosphorylated (lanes 1–3) or phosphorylated (lanes 4–6) forms of the truncated RLC. Following phosphorylation of RLC by MLCK, binding of myosin RLC (MRLC 1–129) to MDR1 was lost (panel C). Binding of myosin RLC (MRLC 1–129) to the C-terminus of NMDAR1 was also decreased relative to the non-phosphorylated state (panel D). Panels C and D are each representative of three independent determinations.

for full-length RLC (data not shown). Thus, phosphorylation of critical residues in the amino terminus of the light chain disrupts binding to both MDR1 and NMDAR1. Our previous study of NMDAR2A revealed the same binding pattern [18], indicating that RLC binding to at least three proteins can be disrupted by MLCK-induced phosphorylation. Furthermore, these interactions are inconsistent with the conventional interaction of myosin RLC with myosin II heavy chain in that the RLC remains bound to the heavy chain throughout the actin-myosin ATPase cycle [22].

3.4. Apical-to-basal transport of [³H]-digoxin is enhanced by an inhibitor of MLCK

Although myosin RLC interactions have been implicated in movement of diverse non-myosin targets [6,18] it is not clear if the light chain and MDR1 are in close enough proximity in whole cells to influence drug transport. To study a potential influence of myosin RLC on MDR1 physiology, we investigated the transport of [³H]-digoxin, a well-known MDR1 substrate, in MDCKII-MDR1 cells. MDCK-type epithelial cells are able to polarize in culture and are widely used as a model system to evaluate MDR1-mediated transport of drugs. Cell monolayers, grown on semipermeable supports, were pretreated with either ML-7 (10 μM), a pharmacological inhibitor of MLCK [28,29], or verapamil (100 μM), a direct inhibitor of MDR1 function. Transepithelial transport of [³H]-digoxin (1 μCi; 0.5 μM) was then assessed across MDCKII-MDR1 monolayers in the absence of inhibitor in both AP to BL and BL to AP directions.

ML-7 caused a significant increase in AP to BL permeability of [³H]-digoxin that was generally sustained for the duration of the three-hour study (Fig. 4A and B). In contrast, we observed no significant change in BL to AP permeability of [³H]-digoxin in response to ML-7 (Fig. 4C and data not shown). Effective permeability of [³H]-digoxin was greatest in the first 30 min after ML-7 treatment, with a greater than twofold increase in AP to BL (Fig. 4B), but no significant change in BL to AP permeability (Fig. 4C). In contrast, verapamil induced a significant decrease in BL to AP permeability, with no significant change in AP to BL permeability (Fig. 4B and C). Although ML-7 and verapamil induced distinct patterns in [³H]-digoxin transport, both responses resulted in a decrease in the efflux ratio (P_{app} (BL → AP)/P_{app} (AP → BL)) of the substrate. ML-7-treated cells showed a threefold decrease in the efflux ratio of [³H]-digoxin (2.70 ± 0.59 compared with 8.44 ± 1.09 in vehicle-treated monolayers; $p < 0.01$), which was comparable to that measured with verapamil, a direct inhibitor of MDR1-mediated efflux activity, (3.75 ± 1.29 relative to 6.82 ± 1.09 in vehicle).

Our functional studies are consistent with a scenario whereby MDR1 is closely associated with myosin RLC in MDCK-MDR1 cells. Efflux of drugs that are also MDR substrates contributes to poor bioavailability and failure of numerous therapeutic regimens and thus our findings provide insight into the potential influence of MDR-interacting proteins on transporter function. Analysis of MDR1-RLC interactions support site-specific phosphorylation of amino terminal residues as a mechanism for myosin RLC dissociation, thus a RLC-bound conformation was likely favored in the presence of ML-7. In a previous study, expression of a mutated GFP-tagged RLC in which Thr18 and Ser19 were changed to alanine resulted in decreased apical expression of BSEP in polarized MDCK cells [6]. Taking previous studies of BSEP and NMDA receptor trafficking into account [6,18], it is most likely that ML-7 altered transepithelial transport of [³H]-digoxin herein by directly, or indirectly, perturbing intracellular trafficking of MDR1. However, in contrast to conclusions drawn with BSEP [6], we find that direct RLC-MDR1 interactions are not compatible with conventional myosin II structure.
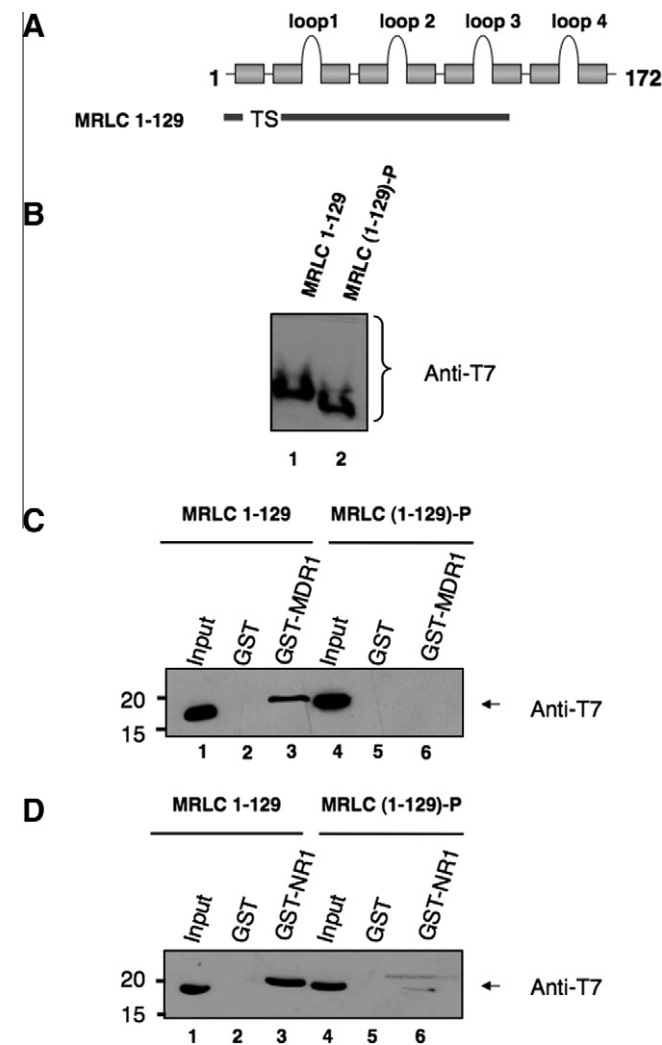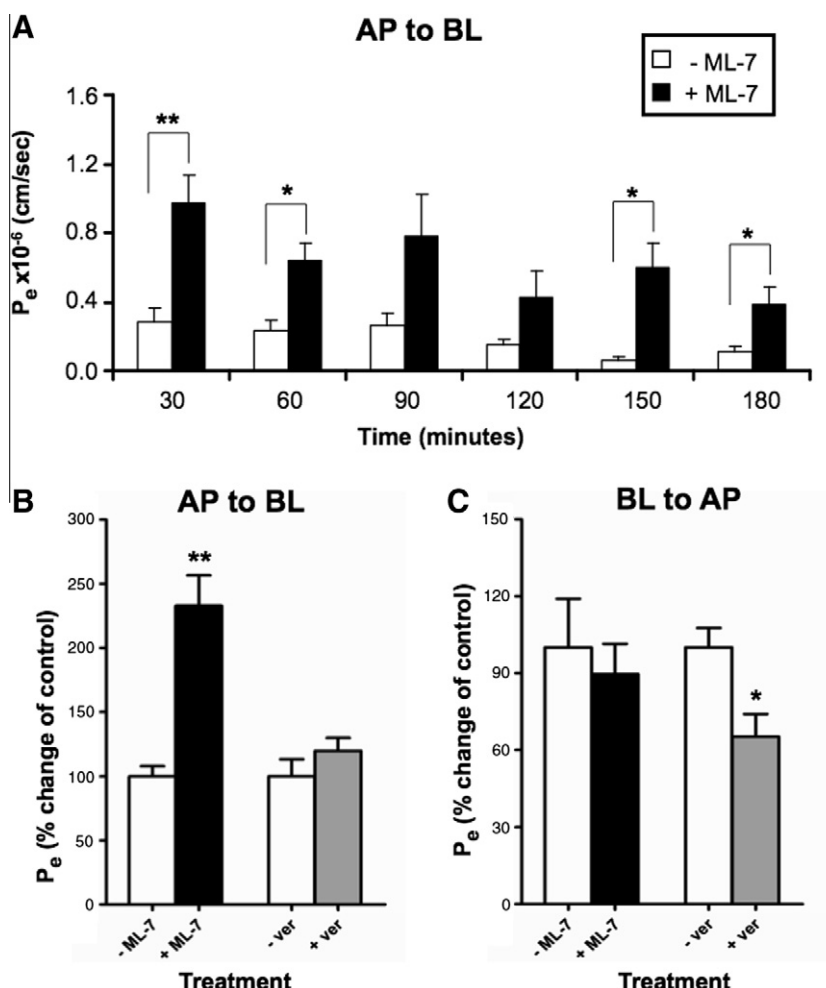
Fig. 4. Apical to basolateral permeability (P_e) of [^{3}H]-digoxin is enhanced in MDCKII-MDR1 cells following inhibition of myosin light chain kinase (MLCK). (A)Histogram shows mean effective permeability coefficient (P_e) of [^{3}H]-digoxin ± SE calculated every 30 min in the apical (AP) to basolateral (BL) direction for 3 h after exposure to vehicle (−ML-7; clear bars) or ML-7 (+ML-7; black bars), a MLCK inhibitor. (B,C) Histograms compare the relative change in [^{3}H]-digoxin effective permeability (P_e) in the AP to BL direction (panel B), or BL to AP direction (panel C), thirty min following exposure to vehicle (clear bars), ML-7 (10 µM; black bars), or verapamil (100 µM; grey bars), a direct inhibitor of MDR1-mediated efflux. *Methods.* For all transepithelial transport studies, permeability of [^{3}H]-digoxin (1 µCi; 0.5 µM) was assessed in polarized, electrically-resistant MDCKII-MDR1 cell monolayers in both AP→BL and BL→AP after pretreatment with pharmacologic inhibitors or vehicle and are expressed as mean ± SE ($n = 3$–4 wells for each time point). Differences between treated and control wells were analyzed using an unpaired *t*-test. Statistical significance is represented as: **$p < 0.01$, *$p < 0.05$.

4. Conclusion

Permeability of digoxin, a widely used cardiac glycoside and MDR1 substrate, was enhanced by pharmacological inhibition of the cytoskeletal motor protein myosin RLC. This finding has implications for pharmacoresistance in that MDR1-interacting partners potentially represent a class of proteins with the ability to modulate drug transport. Although MDR1 can be closely associated with myosin RLC in intact cells, several observations made *in vitro* indicate that myosin RLC binds MDR1 in a non-traditional manner. Binding occurred in the absence of magnesium, via the amino terminal of the RLC, and was inhibited by MLCK-induced phosphorylation, It is therefore unlikely that myosin RLC binds the MDR1 linker region and myosin II heavy chain at the same time.

References

[1] C.J. Chen, J.E. Chin, K. Ueda, D.P. Clark, I. Pastan, M.M. Gottesman, I.B. Roninson, Internal duplication and homology with bacterial transport proteins in the mdr1 (P-glycoprotein) gene from multidrug-resistant human cells, Cell 47 (1986) 381–389.

[2] U.A. Germann, P-glycoprotein – a mediator of multidrug resistance in tumour cells, Eur. J. Cancer 32A (1996) 927–944.

[3] C.A. Hrycyna, L.E. Airan, U.A. Germann, S.V. Ambudkar, I. Pastan, M.M. Gottesman, Structural flexibility of the linker region of human P-glycoprotein permits ATP hydrolysis and drug transport, Biochemistry 37 (1998) 13660–13673.

[4] P.S. Rao, K.B. Mallya, K.S. Srivenugopal, K.C. Balaji, U.S. Rao, RNF2 interacts with the linker region of the human P-glycoprotein, Int. J. Oncol. 29 (2006) 1413–1419.

[5] S.L. Nuti, U.S. Rao, Proteolytic cleavage of the linker region of the human P-glycoprotein modulates its ATPase function, J. Biol. Chem. 277 (2002) 29417–29423.

[6] W. Chan, G. Calderon, A.L. Swift, J. Moseley, S. Li, H. Hosoya, I.M. Arias, D.F. Ortiz, Myosin II regulatory light chain is required for trafficking of bile salt export protein to the apical membrane in Madin–Darby canine kidney cells, J. Biol. Chem. 280 (2005) 23741–23747.

[7] R. Kolling, S. Losko, The linker region of the ABC-transporter Ste6 mediates ubiquitination and fast turnover of the protein, EMBO J. 16 (1997) 2251–2261.

[8] E. Georges, The P-glycoprotein (ABCB1) linker domain encodes high-affinity binding sequences to alpha- and beta-tubulins, Biochemistry 46 (2007) 7337–7342.

[9] D.F. Ortiz, J. Moseley, G. Calderon, A.L. Swift, S. Li, I.M. Arias, Identification of HAX-1 as a protein that binds bile salt export protein and regulates its

abundance in the apical membrane of Madin–Darby canine kidney cells, J. Biol. Chem. 279 (2004) 32761–32770.

[10] D. Amparan, D. Avram, C.G. Thomas, M.G. Lindahl, J. Yang, G. Bajaj, J.E. Ishmael, Direct interaction of myosin regulatory light chain with the NMDA receptor, J. Neurochem. 92 (2005) 349–361.

[11] C. Kioussi, M. Appu, C.V. Lohr, K.A. Fischer, G. Bajaj, M. Leid, J.E. Ishmael, Co-expression of myosin II regulatory light chain and the NMDAR1 subunit in neonatal and adult mouse brain, Brain Res. Bull. 74 (2007) 439–451.

[12] M.A. Conti, R.S. Adelstein, Nonmuscle myosin II moves in new directions, J. Cell Sci. 121 (2008) 11–18.

[13] V.J. Allan, H.M. Thompson, M.A. McNiven, Motoring around the Golgi, Nat. Cell Biol. 4 (2002) E236–242.

[14] A.S. DePina, G.M. Langford, Vesicle transport: the role of actin filaments and myosin motors, Microsc. Res. Tech. 47 (1999) 93–106.

[15] A.S. DePina, T. Wollert, G.M. Langford, Membrane associated nonmuscle myosin II functions as a motor for actin-based vesicle transport in clam oocyte extracts, Cell Motil. Cytoskeleton 64 (2007) 739–755.

[16] E. Ikonen, J.B. de Almeid, K.R. Fath, D.R. Burgess, K. Ashman, K. Simons, J.L. Stow, Myosin II is associated with Golgi membranes: Identification of p200 as nonmuscle myosin II on Golgi-derived vesicles, J. Cell Sci. 110 (Pt 18) (1997) 2155–2164.

[17] A. Musch, D. Cohen, E. Rodriguez-Boulan, Myosin II is involved in the production of constitutive transport vesicles from the TGN, J. Cell Biol. 138 (1997) 291–306.

[18] G. Bajaj, Y. Zhang, M.I. Schimerlik, A.M. Hau, J. Yang, T.M. Filtz, C. Kioussi, J.E. Ishmael, N-Methyl-D-aspartate receptor subunits are non-myosin targets of myosin regulatory light chain, J. Biol. Chem. 284 (2009) 1252–1266.

[19] P.A. Olsson, L. Korhonen, E.A. Mercer, D. Lindholm, MIR is a novel ERM-like protein that interacts with myosin regulatory light chain and inhibits neurite outgrowth, J. Biol. Chem. 274 (1999) 36288–36292.

[20] D. Shafey, J.G. Boyer, K. Bhanot, R. Kothary, Identification of novel interacting protein partners of SMN using tandem affinity purification, J. Proteome Res. 9 (2010) 1659–1669.

[21] M.E. Taub, L. Podila, D. Ely, I. Almeida, Functional assessment of multiple P-glycoprotein (P-gp) probe substrates: influence of cell line and modulator concentration on P-gp activity, Drug Metab. Dispos. 33 (2005) 1679–1687.

[22] P. Crivori, B. Reinach, D. Pezzetta, I. Poggesi, Computational models for identifying potential P-glycoprotein substrates and inhibitors, Mol. Pharm. 3 (2006) 33–44.

[23] I. Rayment, W.R. Rypniewski, K. Schmidt-Base, R. Smith, D.R. Tomchick, M.M. Benning, D.A. Winkelmann, G. Wesenberg, H.M. Holden, Three-dimensional structure of myosin subfragment-1: a molecular motor, Science 261 (1993) 50–58.

[24] A. Houdusse, C. Cohen, Structure of the regulatory domain of scallop myosin at 2 Å resolution: implications for regulation, Structure 4 (1996) 21–32.

[25] M. Terrak, G. Wu, W.F. Stafford, R.C. Lu, R. Dominguez, Two distinct myosin light chain structures are induced by specific variations within the bound IQ motifs-functional implications, EMBO J. 22 (2003) 362–371.

[26] J.R. Boyne, H.M. Yosuf, P. Bieganowski, C. Brenner, C. Price, Yeast myosin light chain Mlc1p, interacts with both IQGAP and class II myosin to effect cytokinesis, J. Cell Sci. 113 (Pt 24) (2000) 4533–4543.

[27] R.S. Moussavi, C.A. Kelley, R.S. Adelstein, Phosphorylation of vertebrate nonmuscle and smooth muscle myosin heavy chains and light chains, Mol. Cell Biochem. 127–128 (1993) 219–227.

[28] M. Saitoh, T. Ishikawa, S. Matsushima, M. Naka, H. Hidaka, Selective inhibition of catalytic activity of smooth muscle myosin light chain kinase, J. Biol. Chem. 262 (1987) 7796–7801.

[29] J. Bain, H. McLauchlan, M. Elliott, P. Cohen, The specificities of protein kinase inhibitors: an update, Biochem. J. 371 (2003) 199–204.